Multivariate classification of complex and multi-echo fMRI data

Scott Peltier, Douglas Noll
Functional MRI Laboratory, Biomedical Engineering
University of Michigan
Ann Arbor, MI USA
spelt@umich.edu

Jonathan Lisinski, Stephen LaConte
Carilion Research Institute
Virginia Tech
Roanoke, VA USA
slaconte@vtc.vt.edu

Abstract— **Multivariate pattern classification and prediction offers an alternative to standard univariate analysis techniques, and has recently been applied in MR imaging using support vector machines (SVM), and used to attain real-time feedback. The standard approach has been to use reconstructed image magnitude data. However, information is also present in the image phase data, and in the k-space data itself. Further, multi-echo imaging offers possibilities of increased functional sensitivity and quantitative imaging. In this study, we explore applying SVM techniques to complex and multi-echo fMRI data, using both phase information and earlier echo-times for prediction.**

Keywords: multivariate, fMRI, complex data, classification

I. INTRODUCTION

Multivariate pattern classification and prediction offers an alternative to standard univariate analysis techniques, and has recently been applied in MR imaging using support vector machines (SVM) [1], and used to attain real-time feedback [2].

The standard approach has been to use reconstructed image magnitude data [3,4]. However, information is also present in the image phase data [5]. A study by Calhoun et al. [6] demonstrated that using the complex image data when performing multivariate ICA resulted in increased detection in number of active voxels as opposed to using magnitude image data alone. Thus, using the information contained in image phase data may be able to predict cognitive states without using the magnitude data.

Classification may also be done on Fourier (k-space) data [7]. This may obviate the need for image reconstruction when performing classification on fMRI data. Subsampling schemes may also be designed, depending on feature localization in k-space, which could make increased temporal sampling possible.

Multi-echo imaging offers possibilities of increased functional sensitivity and quantitative imaging [8-9]. In addition, the use of earlier echo times can help decrease signal loss from susceptibility effects.

This study applies MVPA to complex data in both the image and k-space domains, examining the classification accuracy using both magnitude and phase data. Additionally, complex multi-echo data is also collected, and the classification applied to both early and late echoes.

II. METHODS

A. MR data acquisition and processing

Data were acquired on a 3 T GE scanner. A motor task paradigm was used, with alternating blocks of left and right hand finger tapping (20 s each condition per cycle, 8 cycles total, 320 s total time). Two runs were acquired for each subject.

Study 1: T2*-weighted data were acquired for six subjects using a custom spiral-in sequence. (TR/TE/FA/FOV=2s/30ms/90/22cm, 64x64 matrix, 3mm slice thickness, 40 slices).

Study 2: T2*-weighted data were acquired for five subjects using a custom dual-echo spiral-out sequence, TE1=9.4ms and TE2=30ms, (TR/FA/FOV=2s/90/22cm, 64x64 matrix, 3mm slice thickness, 25 slices).

Image magnitude and phase images were reconstructed for all data. The image phase timecourses were processed to remove phase-wrapping. No other preprocessing was performed on the data.

B. fMRI Classification with Support Vector Machines

The support vector machine (SVM) algorithm is one method for classification used in recent fMRI studies [1-2]. For two classes, the SVM algorithm attempts to find a linear decision boundary (separating hyperplane) using the decision function

$$D(\vec{u}_r) = (\vec{w} \cdot \vec{u}_r) + w_0 \quad (1)$$

where $\vec{w}$ defines the linear decision boundary, and is chosen to maximize the boundaries defined by D = +1 and D = -1 (known as the margin) between the two class distributions.

C. Implemenation and Data analysis

Both SVM training and testing were done using the *3dsvm*

978-0-7695-5061-9/13 $26.00 © 2013 IEEE
DOI 10.1109/PRNI.2013.65

command [1] in AFNI [10]. A soft-margin SVM was used for all data, with a linear kernel and cost function C=100, based on previous work using SVM in fMRI data [1,2]. The classification label (right, left) timecourse was shifted by three samples to account for the hemodynamic response. Six slices covering the bilateral motor cortex were used for analysis.

Classification was performed on run 2 using run 1 as a training data set, and vice versa, and the two accuracy estimates were averaged. Specifically, percent classification accuracy was calculated as [(number of correctly classified images)/(total number of images) × 100]. Classification was done on the magnitude, phase, and complex data in both image space and k-space. In addition, the dependence on k-space coverage was investigated by examining the classification accuracy when using subsets of magnitude k-space.

The SVM analysis was done on the image magnitude, and image phase, for each echotime separately. The images were masked so only voxels inside the brain were analyzed. SVM prediction accuracy was calculated using data from run 1 to test run 2, and vice versa, for echo 1 and echo 2 magnitude and phase data for all subjects.

Visualization of significant features in the SVM analysis was done by inspection of the summed weight vector maps, overlaid on the anatomical images (for image-space data) or the spiral acquisition trajectory (for k-space data).

III. Results

Fig. 1 displays the SVM model weights using the magnitude image data for two slices covering the primary motor cortex. As expected, the significant model weights are located in the primary motor and supplementary motor cortex. The predicted timecourse on the test data shows high accuracy.

Fig. 2 displays the significant model weights and predicted timecourses using image phase data. As can be observed, using raw phase data results in the model weights being concentrated outside the brain, which results in poor prediction on the test run. After brain masking and phase unwrapping, the classification on the corrected phase data yields much higher accuracy, and is comparable to the magnitude results (see Table I).

Classification was also performed using k-space magnitude data. The results using the full k-space or only the central 8th of k-space are very similar, with high classification accuracy, but the accuracy and sensitivity is degraded when using the outer 8th of k-space (see Fig. 3, Table II).

Fig. 4 displays the classification results for the magnitude multi-echo data., and Fig. 5 displays the corresponding phase results. Using the early echo data in either the magnitude or phase data yields high accuracy, and is very comparable to the later echo results (Table III).

IV. Discussion

The classification accuracy was very high in both magnitude k-space and image data. Thus, using k-space data for fMRI classification is feasible, eliminating the need for image reconstruction. This may allow for speed-ups in realtime fMRI (rtfMRI) applications.

The ability to achieve high classification accuracy with only partial k-space coverage can enable faster acquisition approaches. By sacrificing spatial resolution, increased temporal resolution can be obtained. We will investigate these tradeoffs in ongoing work.

The prediction accuracy was very high using the acquired magnitude data at echo 1. Further, the ability to achieve high classification accuracy at multiple echo times may enable alternative acquisition/analysis approaches for real-time fMRI.

The spatial agreement between the significant model weights found using magnitude and phase data respectively is not exact. This may be due to the phase data being more sensitive to large draining veins [5]. Also, the multivariate nature of the model means that the weights for every voxel depend on the values in every other voxel, so some care should be exercised when examining thresholded weight maps.

It is important to also note that no preprocessing besides masking and phase unwrapping was performed on the data for this study. In general, we expect classifier performance could be improved by additional artifact correction. Two main artifact sources are temporal drifts in the magnetic field over time, and modulation of the phase due to physiological noise (particularly respiration). Further work will be done to examine the impact of preprocessing choices on complex-valued fMRI classification.

Another important preprocessing step to be investigated is head motion correction. In the image-space results, the significant model weights are seen to be located in the primary motor cortex, as opposed to being widespread or located more along the edge of the head, which is indicative of head motion. However, in the k-space results it is less clear whether head motion is an influence. Future work will

investigate applying k-space motion correction techniques in order to measure the sensitivity of the k-space classification approach to head motion.

One shortcoming of the present study is that the motor paradigm, while a robust BOLD activation task, does not represent the gamut of possible fMRI tasks. Other cognitive tasks that activate a more disperse network of areas, or have a more subtle BOLD response, will be expected to manifest differently in their phase and k-space responses. Depending on their relative CNR in those domains, they may fall below an acceptable level of accuracy for the classification algorithm. In further work, the use of other experimental paradigms will be employed to gauge the generalizability of the present findings.

V. Conclusions

High classification accuracy was obtained using magnitude image and k-space data. In addition, reduced k-space coverage covering central k-space maintained a high level of accuracy. This can potentially enable rapid real-time classification, without the need for image reconstruction.

The prediction accuracy using the image phase data at either echo time was also very high, and comparable to the image magnitude approach. Phase information can thus be used to augment classification, and classification on images containing reduced BOLD contrast is feasible.

Acknowledgment

This work was supported in part by NIH grants R21/R33 DA026077 (S.P.) and R21/R33 DA026086 (S.L).

References

[1] S.M. LaConte, S. Strother, V. Cherkassky, and X.P. Hu, "Support vector machines for temporal classification of block design fMRI data," NeuroImage, vol. 26, 2005, pp. 317-329.

[2] S.M. LaConte, S.J. Peltier, and X.P. Hu, "Real-time fMRI using brain state classification," Human Brain Mapping, vol. 28, 2007, pp. 1033-1044.

[3] K.A. Norman, S.M. Polyn, G.J. Detre, J.V. Haxby, "Beyond mind-reading: multi-voxel pattern analysis of fMRI data," Trends Cogn Sci., vol.10, 2006, pp. 424-430.

[4] D.D. Cox and R.L. Savoy, "Functional magnetic resonance imaging (fMRI) "brain reading": detecting and classifying distributed patterns of fMRI activity in human visual cortex," Neuroimage, vol. 19, 2003, pp. 261-270.

[5] R. Menon, "Postacquisition suppression of large-vessel BOLD signals in high-resolution fMRI," Magn. Reson. Med., vol. 47, 2002, pp. 1-9.

[6] V.D. Calhoun, T. Adali, G.D. Pearlson, P.C.M. van Zijl, and J.J. Pekar, "Independent component analysis of fMRI data in the complex domain," Magn. Reson. Med., vol. 48, 2002, pp. 180-192.

[7] H. Spies, and I. Ricketts, "Face recognition in Fourier space," Proc. Vision Interface (Vision 2000), 2000, pp.38-44.

[8] S. Posse et al., "Enhancement of BOLD-contrast sensitivity by single-shot multi-echo functional MR imaging," Magn. Reson. Med., vol. 42, 1999, pp. 87-97.

[9] B.A. Poser, M.J. Versluis, J.M. Hoogduin, D.G. Norris, "BOLD contrast sensitivity enhancement and artifact reduction with multiecho EPI: Parallel-acquired inhomogeneity-desensitized fMRI," Magn. Reson. Med., vol. 55, 2006, pp. 1227–1235.

[10] R.W. Cox, "AFNI: software for analysis and visualization of funtional magnetic resonance neruoimages," Comp. and Biomed. Res, vol. 29, 1996, pp. 162-173.

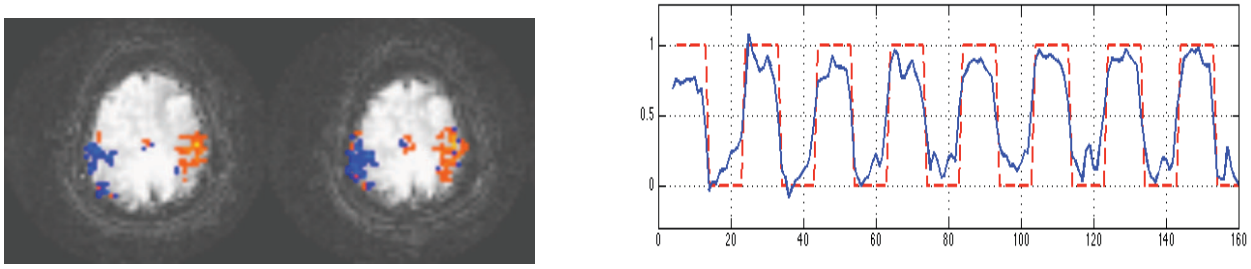

Figure 1. SVM classification output for the magnitude image data, using alternating right-hand (blue) and left-hand (orange) finger tapping.

TABLE I. Classification accuracy using image magnitude and phase data

Subject	Magnitude	Raw phase	Corrected phase
1	0.98	0.53	0.97
2	0.95	0.59	0.85
3	0.93	0.59	0.94
4	0.96	0.63	0.99
5	0.99	0.54	0.95
6	0.93	0.58	0.91

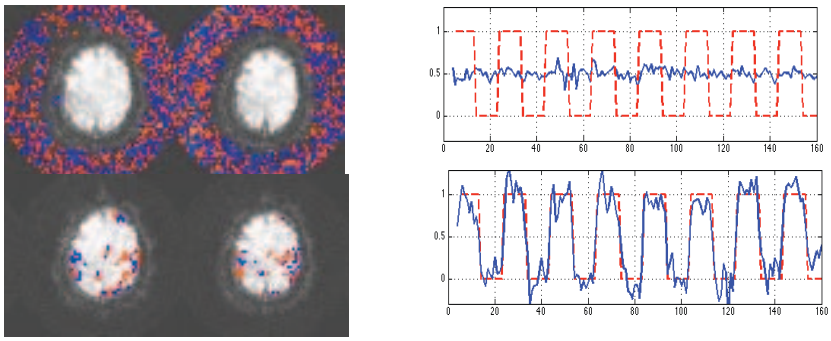

Figure 2. SVM classification output for the phase image data, using alternating right-hand (blue) and left-hand (orange) finger tapping, for raw phase data (top) and unwrapped phase data (bottom).

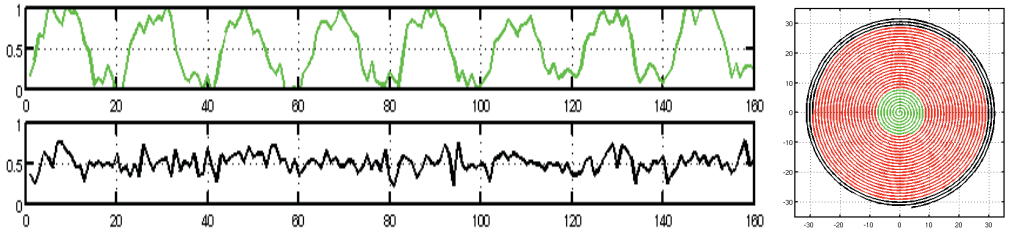

Figure 3. SVM classification output using subsampled k-space.
(Top) Classification prediction using center eighth of k-space. (Bottom) Prediction using outer eighth.

TABLE II. Classification accuracy using magnitude k-space data

Subject	Full k-space	Inner eighth	Outer eighth
1	0.98	0.98	0.74
2	0.92	0.83	0.67
3	0.91	0.93	0.63
4	0.97	0.96	0.65
5	0.97	0.97	0.68
6	0.91	0.92	0.63

TABLE III. Classification accuracy using complex multi-echo data

	Echo 1		Echo 2	
Subject	Mag	Phase	Mag	Phase
1	0.86	0.81	0.98	0.86
2	0.91	0.87	0.95	0.92
3	0.96	0.93	0.96	0.95
4	0.80	0.76	0.87	0.77
5	0.92	0.81	0.98	0.86

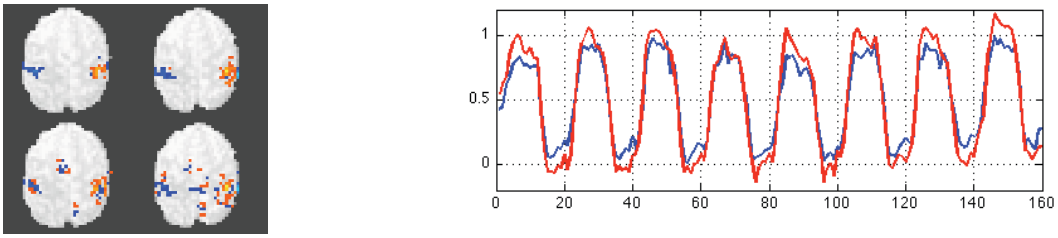

Figure 4. SVM classification output for the multi-echo magnitude image data, using alternating right-hand and left-hand finger tapping, for echo 1 data (bottom, blue plot) and echo 2 data (top, red plot).

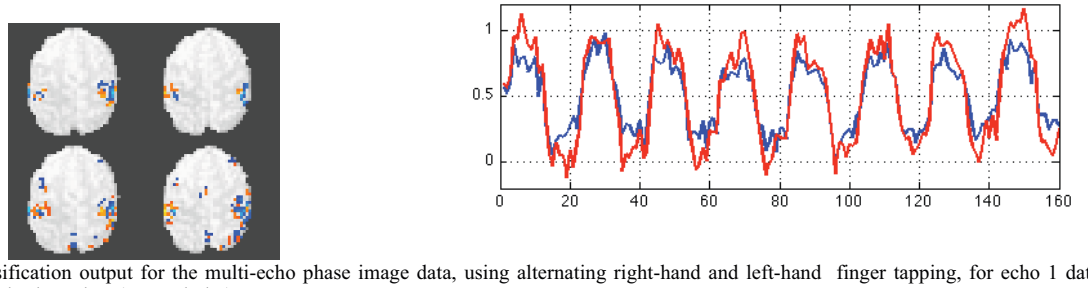

Figure 5. SVM classification output for the multi-echo phase image data, using alternating right-hand and left-hand finger tapping, for echo 1 data (bottom, blue plot) and echo 2 data (top, red plot).